

Reduced Polyoxomolybdates with the Keggin and Dawson Structures: Preparation and Crystal Structures of Two-electron Reduced $[\text{K}(18\text{-crown-6})]_2[\text{N}(\text{PPh}_3)_2]_2[\text{HPMo}_{12}\text{O}_{40}] \cdot 8\text{MeCN} \cdot 18\text{-crown-6}$ and Four-electron Reduced $[\text{NBu}_4]_5^- [\text{H}_3\text{S}_2\text{Mo}_{18}\text{O}_{62}] \cdot 4\text{MeCN}$ (18-crown-6 = 1,4,7,10,13,16-hexaoxa-cyclooctadecane)†

Ralf Neier, Christa Trojanowski and Rainer Mattes*

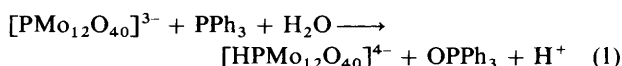
Anorganisch-Chemisches Institut der Westfälischen Wilhelms-Universität, Wilhelm-Klemm-Strasse 8, D-48149 Münster, Germany

By reaction of $[\text{K}(18\text{-crown-6})][\text{N}(\text{PPh}_3)_2]_2[\text{PMo}_{12}\text{O}_{40}] \cdot 2\text{MeCN}$ **1** and $[\text{NBu}_4]_4[\text{S}_2\text{Mo}_{18}\text{O}_{62}]$ with PPh_3 in acetonitrile the new compounds $[\text{K}(18\text{-crown-6})]_2[\text{N}(\text{PPh}_3)_2]_2[\text{HPMo}_{12}\text{O}_{40}] \cdot 8\text{MeCN} \cdot 18\text{-crown-6}$ **2** (18-crown-6 = 1,4,7,10,13,16-hexaoxacyclooctadecane) and $[\text{NBu}_4]_5[\text{H}_3\text{S}_2\text{Mo}_{18}\text{O}_{62}] \cdot 4\text{MeCN}$ **3** were prepared. Compound **2** contains the two-electron reduced $[\text{HPMo}_{12}\text{O}_{40}]^{4-}$ ion having the α -Keggin structure, **3** the four-electron reduced $[\text{H}_3\text{S}_2\text{Mo}_{18}\text{O}_{62}]^{5-}$ ion having the α -Dawson structure. Compounds **1–3** were characterised by means of IR and NMR spectroscopy and X-ray diffraction. The structures of **1** and **2** are disordered in space group $P\bar{1}$. The heteropolyanions show apparent T_h symmetry; their actual symmetry is T . Upon reduction the Mo...Mo distances increase slightly. The strongly alternating 'short' (mean 1.814 Å) and 'long' (1.990 Å) Mo–O–Mo bonds in the unreduced compound **1** become more equal in **2**. The structural changes upon reduction observed in **3** were analysed in detail. The most significant alterations are an increase of the Mo...Mo distances between corner-sharing MoO_6 octahedra in the equatorial belt by 0.066 Å, and a decrease of the Mo–O–Mo bond lengths connecting the two halves of the anion. The alternation of the Mo–O(bridge) bonds is nearly evened out after reduction. All structural changes observed in **2** and **3** are consistent with the description that the additional electrons occupy delocalised molecular orbitals extending over the Mo–O_b framework.

Reduced heteropolyanions ('heteropoly blues') are of continuing interest in important areas of chemistry like analytical and medical applications, catalysis, electron transfer and delocalisation of electrons in mixed-valence compounds. Despite significant evidence obtained by electrochemical studies, and by UV, ESR and multinuclear NMR spectroscopy,^{1–4} structural data are still scarce. Pope and co-workers^{5,6} reported the structure of four-electron reduced β - $[\text{H}_3\text{PMo}_{12}\text{O}_{40}]^{4-}$, Müller *et al.*⁷ the structures of four-electron reduced β - $[\text{H}_4\text{AsMo}_{12}\text{O}_{40}]^{3-}$ and of two-electron reduced α - $[\text{H}_2\text{AsMo}_{12}\text{O}_{40}]^{3-}$. The crystal structure of two-electron reduced α - $[\text{Co}^{\text{II}}\text{W}_{12}\text{O}_{40}]^{8-}$ was elucidated by Baker and co-workers.⁸ Some of these structural studies were hampered by the limited quality of the diffraction data and by disorder. We prepared two-electron reduced α - $[\text{HPMo}_{12}\text{O}_{40}]^{4-}$ and four-electron reduced α - $[\text{H}_3\text{S}_2\text{Mo}_{18}\text{O}_{62}]^{5-}$ by chemical reduction in acetonitrile using PPh_3 as reductant, a method recently described by Kawafune and co-workers.^{9–11} We present here the results of analytical, spectroscopic and low-temperature single-crystal X-ray studies of these species. The X-ray data allow a more complete description of the structural changes occurring upon reduction of heteropolyoxomolybdates. To our knowledge, reduced heteropolymetalates with Dawson structures have not been structurally characterised so far.

Results and Discussion

Preparation.—The reduction of polyoxomolybdates with Keggin and Dawson structure by triphenylphosphine in non-aqueous solutions under anaerobic conditions is a very convenient method. The ion $[\text{PMo}_{12}\text{O}_{40}]^{3-}$ undergoes stoichiometric reduction by PPh_3 , accompanied by oxygen transfer to PPh_3 .^{10,11} However, in contrast to Kawafune, we suggest that the overall structure of the anion remains unchanged. The transferred oxygen atoms are immediately replaced in the polyanion according to equation (1).



Applying large organic counter ions like $[\text{N}(\text{PPh}_3)_2]^+$, $[\text{K}(18\text{-crown-6})]^+$ (18-crown-6 = 1,4,7,10,13,16-hexaoxacyclooctadecane) or $[\text{NBu}_4]^+$ we obtained well defined compounds in good yields as X-ray-quality crystals from acetonitrile. Thus reaction of $[\text{K}(18\text{-crown-6})][\text{N}(\text{PPh}_3)_2]_2[\text{PMo}_{12}\text{O}_{40}] \cdot 2\text{MeCN}$ **1** yields the two-electron reduced heteropolyoxomolybdate $[\text{K}(18\text{-crown-6})]_2[\text{N}(\text{PPh}_3)_2]_2[\text{HPMo}_{12}\text{O}_{40}] \cdot 8\text{MeCN} \cdot 18\text{-crown-6}$ **2** having the Keggin structure, and that of $[\text{NBu}_4]_4[\text{S}_2\text{Mo}_{18}\text{O}_{62}]$ gives the four-electron reduced heteropoly oxomolybdate $[\text{NBu}_4]_5[\text{H}_3\text{S}_2\text{Mo}_{18}\text{O}_{62}] \cdot 4\text{MeCN}$ **3** having the Dawson structure. The degree of reduction was determined by several independent methods. Volumetric titration with cerium(IV) sulfate showed that for $[\text{HPMo}_{12}\text{O}_{40}]^{4-}$ a two-electron reduction had taken place per formula unit and for $[\text{H}_3\text{S}_2\text{Mo}_{18}\text{O}_{62}]^{5-}$ a four-electron reduction. In the ³¹P NMR spectrum of $[\text{HPMo}_{12}\text{O}_{40}]^{4-}$

† Supplementary data available: see Instructions for Authors, *J. Chem. Soc., Dalton Trans.*, 1995, Issue 1, xxv–xxx.

the signal of the heteroatom phosphorus shifts from δ 0.89 for $[\text{PMo}_{12}\text{O}_{40}]^{3-}$ to δ -2.02, with the signal for the $[\text{N}(\text{PPh}_3)_2]^+$ ion constant at δ 25.52 as internal standard for both compounds. Similar upfield shifts have been observed earlier and assigned to a two-electron reduced species $[\text{H}_n\text{PMo}_{12}\text{O}_{40}]^{(5-n)-}$.¹¹

The UV/VIS spectrum of $[\text{PMo}_{12}\text{O}_{40}]^{3-}$ shows no absorption in the range of d-d transitions. However, that of $[\text{HPMo}_{12}\text{O}_{40}]^{4-}$ displays a wide absorption band with the maximum at 727 nm and an absorption coefficient $\epsilon = 380 \text{ dm}^3 \text{ mol}^{-1} \text{ cm}^{-1}$. The intensity of this intervalence charge-transfer band has been reported to be proportional to the number of electrons introduced into the polyanion.¹¹ An absorption coefficient of this magnitude corresponds to a reduction by 1.8 to 2 electrons. Independently from the volumetric redox titration, the four-electron reduction of $[\text{H}_3\text{S}_2\text{Mo}_{18}\text{O}_{62}]^{5-}$ was corroborated by the structural data (see below). Unlike all other heteropolyanions, Dawson-type heteropolymolybdates have long been believed to undergo only even-numbered electron reductions.^{12a} However, very recently the first odd oxidation level Dawson heteropolymolybdates $[\text{P}_2\text{Mo}_{18}\text{O}_{62}]^{7-}$ and $[\text{S}_2\text{Mo}_{18}\text{O}_{62}]^{5-}$ have been identified.^{12b-d} No ^{95}Mo or ^{17}O NMR data could be obtained for **2** and **3** due to the limited solubility of these compounds and the relative sensitivity of these nuclei.

Infrared Spectra.—The IR spectra of $[\text{PMo}_{12}\text{O}_{40}]^{3-}$, $[\text{HPMo}_{12}\text{O}_{40}]^{4-}$, $[\text{S}_2\text{Mo}_{18}\text{O}_{62}]^{4-}$ and $[\text{H}_3\text{S}_2\text{Mo}_{18}\text{O}_{62}]^{5-}$ are shown in Figs. 1 and 2. In the first pair of compounds the spectrum of the reduced species is significantly different from that of the unreduced species. The relative intensities of the peaks at 809, 881 and 1062 cm^{-1} decrease considerably after reduction. The first two absorptions have to be assigned to the antisymmetric Mo–O–Mo stretching vibrations of corner- and edge-sharing MoO_6 octahedra, the last one to the three-fold degenerate P–O(–Mo) vibration.¹³ According to Kawafune and co-workers⁹⁻¹¹ the decrease in intensity is caused by elimination of oxygen atoms from the $\text{Mo}^{\text{VI}}\text{–O–Mo}^{\text{VI}}$ bonds to produce two neighbouring molybdenum(v) ions in an incomplete Keggin ion. We do not agree with this conclusion. All chemical and structural evidence shows that the Keggin structure $\text{PMo}_{12}\text{O}_{40}$ remains intact after reduction.¹⁻⁸ The loss in intensity is rather due to the smaller transition moment for the vibrations under discussion. The transition moment decreases because the molybdenum–oxygen bridge bonds, which are alternating ‘short’ and ‘long’ in $[\text{PMo}_{12}\text{O}_{40}]^{3-}$, become more equal in $[\text{HPMo}_{12}\text{O}_{40}]^{4-}$ and because the additional electrons occupy delocalised orbitals. The Mo=O stretching vibration (O_t is a terminally bonded oxygen atom) at 956 cm^{-1} is not affected by the reduction.

For the species $[\text{S}_2\text{Mo}_{18}\text{O}_{62}]^{4-}$ and $[\text{H}_3\text{S}_2\text{Mo}_{18}\text{O}_{62}]^{5-}$ the intensity of the absorption bands in the region of the Mo–O–Mo bridging vibrations (700–900 cm^{-1}) changes even more dramatically for the reasons just mentioned. Owing to the lower symmetry of $[\text{S}_2\text{Mo}_{18}\text{O}_{62}]^{4-}$ the S–O vibration is split into two components. In $[\text{H}_3\text{S}_2\text{Mo}_{18}\text{O}_{62}]^{5-}$ further splitting is observed. The most intense band is shifted from 1170 to 1156 cm^{-1} . At the same time the broad bands of the Mo–O–Mo bridging vibrations move to lower frequencies. These observations will be discussed below in the context of the structural results.

The Crystal Structures.—(a) $[\text{PMo}_{12}\text{O}_{40}]^{3-}$. The unit cell of compound **1** contains two independent, nearly identical $[\text{PMo}_{12}\text{O}_{40}]^{3-}$ ions, located at the inversion centres 000 and $\frac{1}{2}\frac{1}{2}0$, four $[\text{N}(\text{PPh}_3)_2]^+$ ions, and two $[\text{K}(18\text{-crown})(\text{MeCN})_2]^+$ ions with the potassium atoms located at $0\frac{1}{2}0$ and $\frac{1}{2}00$. The polymolybdate ions form a centred arrangement in the *ab* plane together with the potassium ions. The site symmetry $\bar{1}$ is incompatible with the tetrahedral symmetry of the Keggin structure. Therefore the structure of **1** shows the central P atom surrounded by a cube of eight oxygen atoms and the Mo atoms

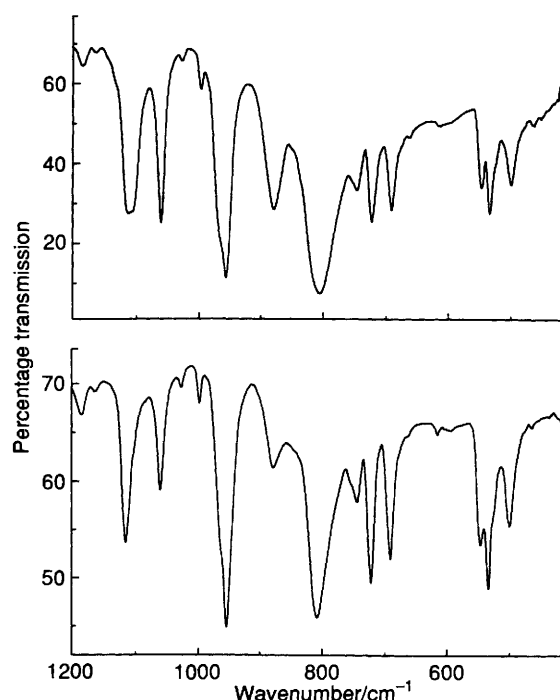


Fig. 1 Infrared spectra of $[\text{PMo}_{12}\text{O}_{40}]^{3-}$ (top) and $[\text{HPMo}_{12}\text{O}_{40}]^{4-}$ (bottom)

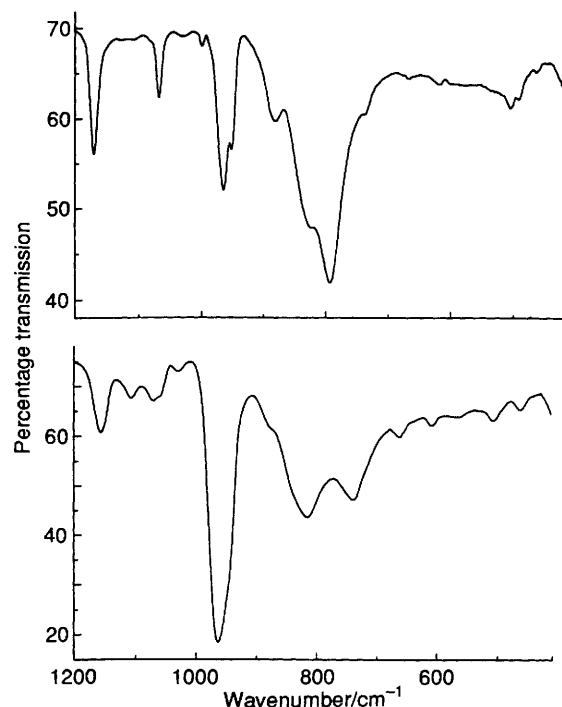


Fig. 2 Infrared spectra of $[\text{S}_2\text{Mo}_{18}\text{O}_{62}]^{4-}$ and $[\text{H}_3\text{S}_2\text{Mo}_{18}\text{O}_{62}]^{5-}$ (bottom)

situated at the corners of a regular cubooctahedron. All $\text{Mo}\cdots\text{Mo}$ distances are equal, although they are different between edge- and corner-sharing octahedra in a single Keggin anion. The vibrational ellipsoids of all oxygen atoms have very characteristic shapes: those of bridging oxygen atoms are elongated radially, whereas those of terminal oxygen atoms are either flattened or tangentially extended (see Fig. 3). Evans and Pope¹⁴ have pointed out that a crystallographic result like this can be explained by disorder: a single Keggin anion is self-superimposed by a second one, which is rotated 90° about a $\bar{4}$

axis. However, this type of disorder does not explain completely the present structural results. Polyoxomolybdates with Keggin structures lack $T_d(\bar{4}3m)$ symmetry; the symmetry is lowered to $T(23)$, a chiral point group.^{1,15} This arises from small displacements of the Mo atoms within their MoO_6 octahedra, which result in alternating 'long' and 'short' Mo–O–Mo bonds. The symmetry operation mentioned above would average these 'long' and 'short' bonds, contrary to our results, where the Mo–O–Mo bonds fall into two well resolved categories: 1.790(9)–1.843(9) (mean 1.814) and 1.962(9)–2.019(7) (mean 1.990) Å.

We propose the following model to explain these observations. The single anion $[\text{PMo}_{12}\text{O}_{40}]^{3-}$ is chiral. Both enantiomers, which are related to each other by a mirror operation, exist in equal amounts. If they are located at the same site of the unit cell and crystallographically superimposed, they appear as a pseudo-molecule which belongs to the centrosymmetric point group $T_h(2/m\bar{3})$. The alternating 'short' and 'long' Mo–O–Mo bonds are then retained, but edge- and corner-shared MoO_6 octahedra are superimposed. The recently published structure of $[\text{Fe}(\text{C}_5\text{Me}_5)_2]_4[\text{SiMo}_{12}\text{O}_{40}]\cdot\text{dmf}$ (dmf = dimethylformamide) shows exactly the same type of disorder with retention of alternating Mo–O–Mo bonds.*

Table 1 contains a summary of the most significant bond distances and angles of $[\text{PMo}_{12}\text{O}_{40}]^{3-}$. Despite the disorder the structure is discussed in some detail in order to evaluate the obvious structural changes upon reduction. Chemically identical bond distances and angles vary only slightly with the exception of Mo–O(P) and P–O(Mo) bonds. Literature data give Mo...Mo distances of 3.41 Å for bonds within a triplet of edge-shared MoO_6 octahedra and of 3.71 Å for bonds between triplets (corner-shared MoO_6 octahedra).¹ The average value is 3.56 Å. A recent publication, where $\bar{4}3m$ symmetry has been proposed for $[\text{VMo}_{12}\text{O}_{40}]^{3-}$,¹⁶ gives the following distances: Mo...Mo 3.324(2) and 3.674(2) Å (mean 3.499 Å), Mo–O_t 1.665(9) Å, Mo–O_b 1.902(9) within the triplets and 1.928(5) Å between the triplets. In $[\text{Fe}(\text{C}_5\text{Me}_5)_2]_4[\text{SiMo}_{12}\text{O}_{40}]$ the mean Mo...Mo distance is 3.522 Å.⁴ In comparison to these values the mean Mo...Mo distance in **1**, 3.569 Å, is slightly larger. The Mo–O_t bonds tend also to be larger than in the reference data {with the exception of $[\text{Fe}(\text{C}_5\text{Me}_5)_2]_4[\text{SiMo}_{12}\text{O}_{40}]$ }. We ascribe this to the predominant hydrophobic environment of the Keggin ion in the crystal lattice of **1**. The Mo–O–Mo bonds are strongly asymmetric as already mentioned. In the reference structures the bridging oxygen atoms participate in hydrogen bonds. Therefore the asymmetry of the Mo–O–Mo bonds, ranging from 1.85 to 1.97 Å, is less expressed.

(b) $[\text{HPMo}_{12}\text{O}_{40}]^{4-}$. The unit cell of compound **2** contains one reduced Keggin ion, located at the inversion centre $0\frac{1}{2}0$, two $[\text{K}(18\text{-crown-6})(\text{MeCN})]^+$ ions and two $[\text{N}(\text{PPh}_3)_2]^+$ ions; six unco-ordinated MeCN molecules and one empty 18-crown-6 molecule at $\frac{1}{2}\frac{1}{2}\frac{1}{2}$ complete the contents of the unit cell. According to the analytical results, **2** is a two-electron reduced species. It then carries the charge 5–. To reach electroneutrality within the structure, the presence of one proton has to be inferred. The most probable location is at one of the 24 bridging oxygen atoms.^{1–8} The Keggin anion of **2** shows exactly the same disorder as described previously. The magnitude of the thermal displacement parameters of the Mo and the three groups of O atoms, and the orientation of the vibrational ellipsoids, are very similar in both structures (see Fig. 4). Baker and co-workers⁹ noticed, on the contrary, a marked decrease of the displacement parameters upon reduction of $\alpha\text{-}[\text{Co}^{\text{II}}\text{W}_{12}\text{O}_{40}]^{4-}$. Despite the disorder the structural data show a high degree of precision for both compounds. It is legitimate, therefore, to compare the structures of $[\text{PMo}_{12}\text{O}_{40}]^{3-}$ and $[\text{HPMo}_{12}\text{O}_{40}]^{4-}$ in order to evaluate the changes caused by reduction.

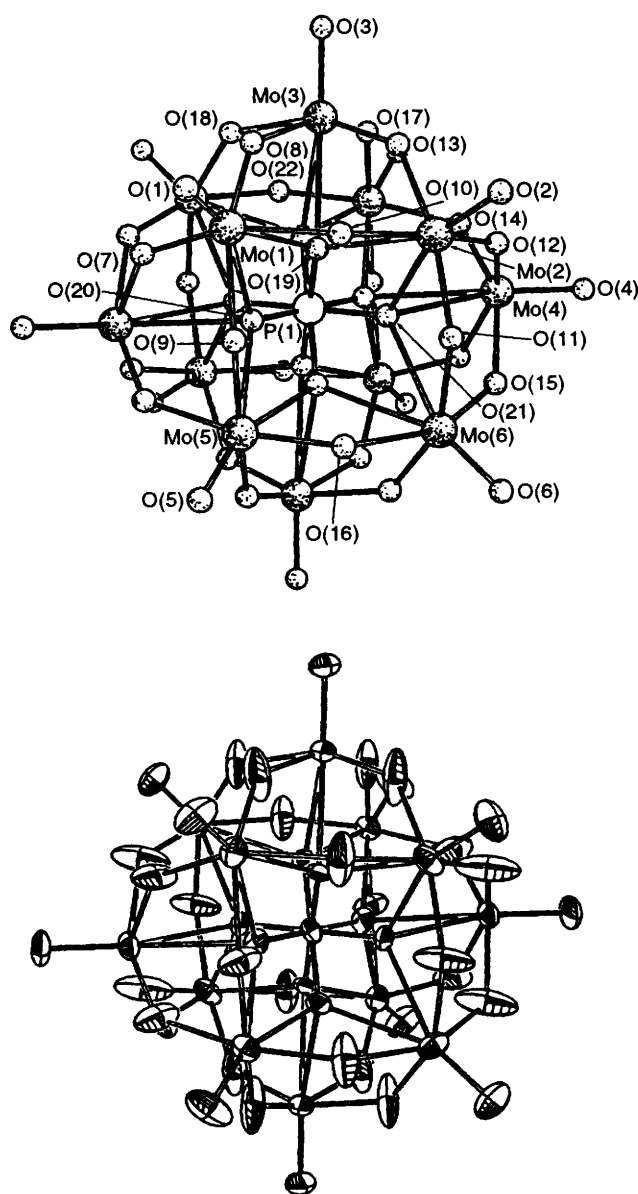


Fig. 3 Structure of $[\text{PMo}_{12}\text{O}_{40}]^{3-}$ displaying atomic labelling and vibrational ellipsoids (50% probability)

The anion $[\text{HPMo}_{12}\text{O}_{40}]^{4-}$ displays the α -Keggin structure like the starting material. Fruchart and Souchay¹⁷ have shown that reduction of $\alpha\text{-}[\text{Mo}_{12}\text{O}_{40}]^{3-}$ in aqueous solutions gives heteropoly blues possessing the β -Keggin structure. This has been confirmed by Pope and co-workers⁵ for $\text{Ca}_{0.5}\text{H}_6\text{P-Mo}_{12}\text{O}_{40}\cdot\text{ca.}18\text{H}_2\text{O}$ by X-ray analysis. Obviously reduction in non-aqueous solutions, as in our case, leads to the more symmetrical α -type anions. The following significant structural changes in $[\text{HPMo}_{12}\text{O}_{40}]^{4-}$ can be detected (see Table 1): the metal atom framework expands slightly from the anion's centre; the alternating 'long' and 'short' Mo–O_b bonds become more equal, but the deviation from equivalence is still significant. In this connection the size of the O_b–Mo–O_b(*cis*) bond angle varies much less in $[\text{HPMo}_{12}\text{O}_{40}]^{4-}$. The M=O_t bond lengths remain unaffected. In the disordered structures of **1** and **2** four least-squares planes can be calculated, which comprise six metal atoms each. The average mean deviation from these planes is much smaller in $[\text{HPMo}_{12}\text{O}_{40}]^{4-}$ (0.024 Å) than in $[\text{PMo}_{12}\text{O}_{40}]^{3-}$ (0.155 Å).

All changes observed are consistent with the description that the two additional electrons occupy tangentially oriented

* The authors of ref. 4 describe the disorder as caused by the mechanism reported in ref. 14.

Table 1 Comparison of bond distances (Å) and angles (°) in $[\text{PMo}_{12}\text{O}_{40}]^{3-}$ and $[\text{HPMo}_{12}\text{O}_{40}]^{4-}$ (mean values in square brackets)

	$[\text{PMo}_{12}\text{O}_{40}]^{3-}$		$[\text{HPMo}_{12}\text{O}_{40}]^{4-}$	
Mo...Mo	3.553(2)–3.587(2)	[3.569(1)]	3.548(2)–3.594(2)	[3.573(1)]
Mo...P	3.549(2)–3.576(2)	[3.558(1)]	3.564(2)–3.586(2)	[3.573(1)]
Mo–O _l	1.641(8)–1.663(8)	[1.654(2)]	1.651(9)–1.669(7)	[1.659(4)]
Mo–O _b ('short')	1.790(9)–1.843(9)	[1.814(2)]	1.859(9)–1.910(6)	[1.888(3)]
Mo–O _b ('long')	1.962(9)–2.019(7)	[1.990(2)]	1.897(13)–1.936(10)	[1.920(3)]
Mo–O(P)	2.403(10)–2.520(9)	[2.471(3)]	2.397(14)–2.576(15)	[2.491(4)]
P–O	1.482(9)–1.578(14)	[1.535(3)]	1.443(14)–1.608(16)	[1.526(4)]
O _b –Mo–O _b (<i>cis</i>) ^a	94.9(4)–97.6(4)	[96.4(2)]	87.6(4)–91.7(5)	[89.6(4)]
O _b –Mo–O _b (<i>cis</i>) ^b	78.1(4)–81.2(4)	[79.9(2)]	84.7(4)–87.0(4)	[85.1(4)]
Mo–O _b –Mo	137.8(6)–141.1(7)	[139.5(1)]	137.7(4)–140.5(6)	[139.6(2)]

^a Between 'short' bonds. ^b Between 'long' bonds.

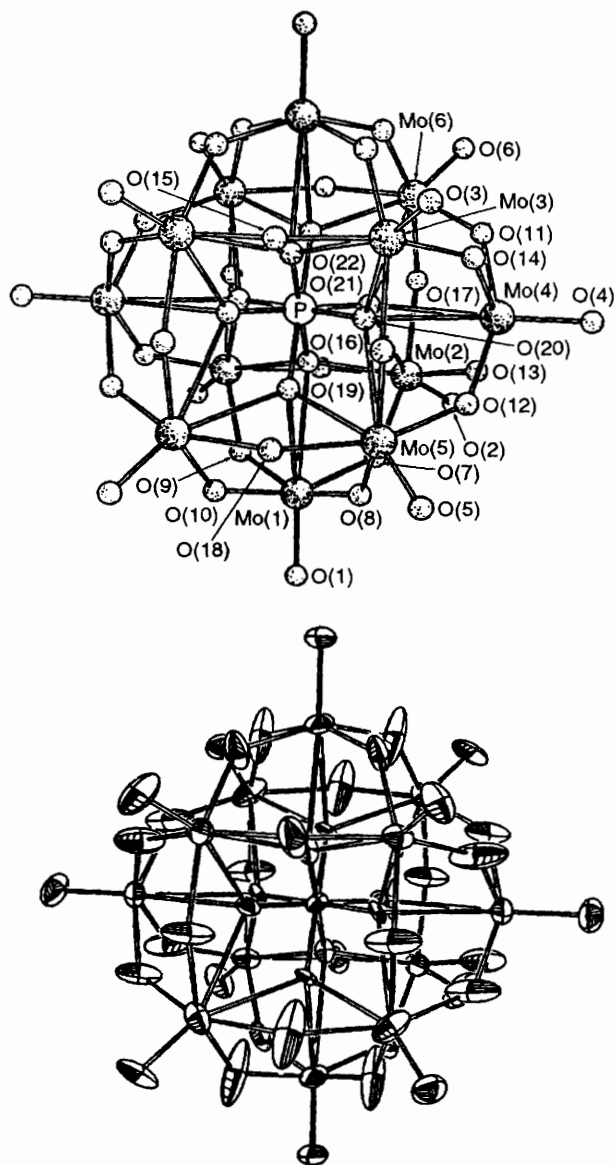


Fig. 4 Structure of $[\text{HPMo}_{12}\text{O}_{40}]^{4-}$ displaying atomic labelling and vibrational ellipsoids (50% probability)

delocalised and non-bonding molecular orbitals.^{1–3,8} Owing to the disorder no differentiation can be made between the bonds within the triplets (edge-sharing octahedra) and the bonds connecting the triplets (corner-sharing octahedra). These two kinds of distances may behave differently upon reduction.

However, the observed similarity of the atomic displacement parameters in $[\text{PMo}_{12}\text{O}_{40}]^{3-}$ and $[\text{HPMo}_{12}\text{O}_{40}]^{4-}$ limits such distinction strongly.

(c) $[\text{H}_3\text{S}_2\text{Mo}_{18}\text{O}_{62}]^{5-}$. Compound 3 crystallises in space group $C2/c$ with four formula units; besides the polyanion, which is located upon a two-fold axis, the unit cell contains 20 $[\text{NBu}^n_4]^+$ ions and 16 MeCN molecules. The anion is not disordered. Considering the analytical results three protons are afforded for electroneutrality. Their locations were determined (see below). The crystal structure of the oxidised S_2Mo_{18} ion (in $[\text{NEt}_4]_4[\text{S}_2\text{Mo}_{18}\text{O}_{62}]\cdot\text{MeCN}$) has been reported recently.¹⁸ So the alterations occurring upon the four-electron reduction can be analysed in detail. The anions $[\text{S}_2\text{Mo}_{18}\text{O}_{62}]^{4-}$ and $[\text{H}_3\text{S}_2\text{Mo}_{18}\text{O}_{62}]^{5-}$ both display the α -Dawson structure (see Fig. 5). In Table 2 the range and/or mean values for chemically identical interatomic distances are given. The following discussion refers in general to the mean values.

The overall symmetry of $[\text{H}_3\text{S}_2\text{Mo}_{18}\text{O}_{62}]^{5-}$ approaches closely D_{3h} . The strongest changes upon reduction take place in the two equatorial belts of edge- and corner-sharing MoO_6 octahedra. The Mo...Mo distance between corner-sharing MoO_6 octahedra increases from 3.693(2) to 3.759(1) Å, whereas the distance between edge-sharing octahedra remains nearly constant at 3.45 Å. The puckering of the Mo atoms in these belts is much less pronounced than in $[\text{S}_2\text{Mo}_{18}\text{O}_{62}]^{4-}$. The mean deviation from the least-squares planes decreases from 0.18 to 0.007 Å. The lengths of the Mo–O_b bonds within the belts, which alternate considerably in $[\text{S}_2\text{Mo}_{18}\text{O}_{62}]^{4-}$, are completely evened out upon reduction and increase slightly. The lateral Mo...S and Mo–O(S) distances also grow with the expansion of the belts.

Within the triplets of edge-sharing Mo_6 octahedra at the top and the bottom of the Dawson structure the following changes occur: the alternation of the Mo–O_b bond lengths, which is very distinct in $[\text{S}_2\text{Mo}_{18}\text{O}_{62}]^{4-}$ with 1.827(5) and 2.000(5) Å for the 'long' and 'short' bonds, respectively, nearly disappears; this contrasts two-electron reduced $[\text{HPMo}_{12}\text{O}_{40}]^{4-}$ where the Mo–O–Mo bonds remain significantly unequal. The mean Mo–O_b bond length and the Mo...Mo distance increase by 0.028 Å to 1.930(3) Å and by 0.014 Å to 3.450(1) Å, respectively.

The Mo...Mo distances along the bridges between triplets and equatorial belts vary in $[\text{S}_2\text{Mo}_{18}\text{O}_{62}]^{4-}$ from 3.681(3) to 3.785(3) Å and in $[\text{H}_3\text{S}_2\text{Mo}_{18}\text{O}_{62}]^{5-}$ from 3.726(1) to 3.836(1) Å. The spread in $[\text{S}_2\text{Mo}_{18}\text{O}_{62}]^{4-}$ is caused by severe puckering in the equatorial belt,¹⁸ but in $[\text{H}_3\text{S}_2\text{Mo}_{18}\text{O}_{62}]^{5-}$ predominantly by a rotation of the triplets *versus* the belt. The Mo–O_b distances in this part of the anion, which alternate in $[\text{S}_2\text{Mo}_{18}\text{O}_{62}]^{4-}$ as usual, show interesting details in $[\text{H}_3\text{S}_2\text{Mo}_{18}\text{O}_{62}]^{5-}$ (see Table 3): the two bonds originating at each of the Mo atoms in the triplets differ by 0.06 Å. All bonds originating at the Mo atoms in the central belt are larger than those originating at the triplets; the difference of 0.102 Å is highly significant. This may signal that the additional electrons preferentially populate orbitals

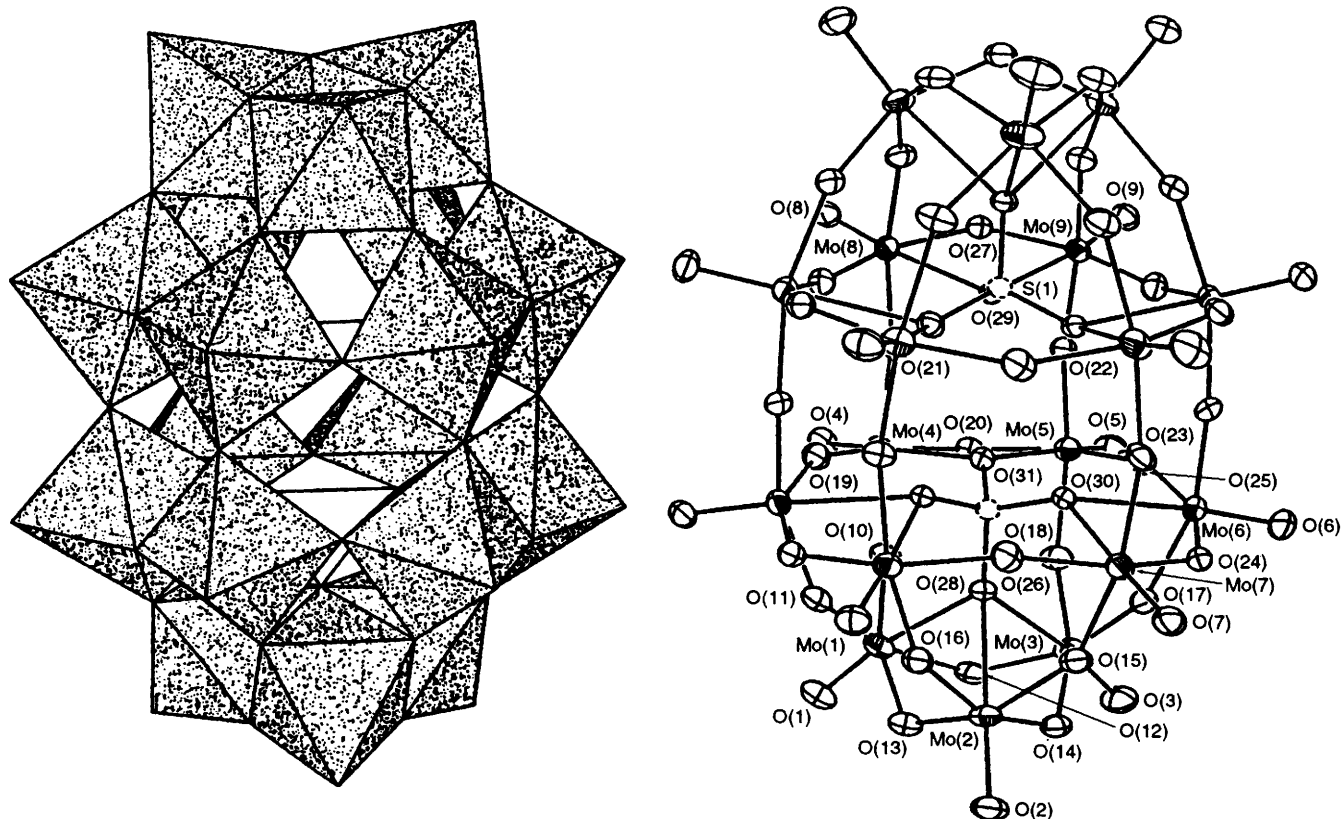


Fig. 5 Structure of $[\text{H}_3\text{S}_2\text{Mo}_{18}\text{O}_{62}]^{5-}$. Polyhedral representation (left), atomic labelling and vibrational ellipsoids (right) (50% probability)

Table 2 Comparison of bond distances (Å) and bond angles ($^\circ$) in $[\text{S}_2\text{Mo}_{18}\text{O}_{62}]^{4-}$ and $[\text{H}_3\text{S}_2\text{Mo}_{18}\text{O}_{62}]^{5-}$ (mean values in square brackets)

		$[\text{S}_2\text{Mo}_{18}\text{O}_{62}]^{4-}$		$[\text{H}_3\text{S}_2\text{Mo}_{18}\text{O}_{62}]^{5-}$	
Mo...Mo _c ^a	within triplets	3.422(3)–3.444(3)	[3.436(2)]	3.432(1)–3.461(1)	[3.450(1)]
	within belts	3.438(3)–3.456(3)	[3.448(2)]	3.447(1)–3.461(1)	[3.455(1)]
Mo...Mo _c ^a	within belts	3.685(3)–3.700(3)	[3.693(2)]	3.747(1)–3.767(1)	[3.759(1)]
	between belts and triplets	3.681(3)–3.785(3)	[3.737(2)]	3.726(1)–3.836(1)	[3.772(1)]
	between belts	3.791(3)–3.805(3)	[3.801(2)]	3.732(1)–3.743(1)	[3.736(1)]
Mo...S	axial	3.586(5)–3.593(4)	[3.595(2)]	3.582(1)–3.602(1)	[3.590(1)]
	lateral	3.514(5)–3.599(5)	[3.569(2)]	3.597(1)–3.639(1)	[3.609(1)]
S...S		3.918(7)		3.922(1)	
S–O		1.421(1)–1.521(1)	[1.471(4)]	1.461(3), 1.464(3), 1.470(4), 1.498(4)	
Mo–O(S)	axial	2.43–2.53	[2.472(4)]	2.473(3)–2.495(4)	[2.485(2)]
	lateral			2.487(3)–2.531(4)	[2.507(2)]
Mo–O _i		1.621(1)–1.691(1)	[1.659(3)]	1.674(4)–1.689(5)	[1.683(1)]
Mo–O _c	within triplets				
	‘short’		[1.827(5)]	1.906(4)–1.929(4)	[1.914(3)]
	‘long’		[2.000(5)]	1.917(4)–1.966(4)	[1.947(3)]
	within belts ^b		[1.872(5)], [1.945(5)]	1.895(4)–1.913(4)	[1.930(3)]
Mo–O _c	within belts ^b		[1.867(5)], [1.933(5)]	1.915(4)–1.934(4)	[1.924(1)]
	triplet–belt ^b		[1.798(4)], [2.015(4)]	(see Table 3)	
	belt–belt ^b		[1.792(4)], [2.045(4)]	1.868(4)–1.892(4)	[1.882(2)]

^a Mo_c and O_c denote distances in corner-sharing, Mo_e and O_e in edge-sharing octahedra. ^b Mean values for ‘short’ and ‘long’ bonds, respectively.

within the central belt. Special attention is merited by the observation that the six Mo–O bonds involving the O atoms O(11), O(15) and O(18) are the longest in each group. We

assume that the three protons, which are required for charge balance, are located there and at the three symmetrically equivalent positions in statistical disorder. Calculations using

bond length–bond strength relations corroborate this assumption. The location of the protons demonstrates that the negative charge increases at these oxygen atoms upon reduction.

It is interesting that the Mo...Mo distances along the bonds which connect the two halves of the anion decrease by 0.065 Å upon reduction. So this type of Mo...Mo distance becomes the shortest one within the three topologically different groups of corner-sharing octahedra, whereas it is the longest one in $[\text{S}_2\text{Mo}_{18}\text{O}_{62}]^{4-}$. The Mo–O_b bond distances decrease at the same time from 1.919(5) to 1.882(2) Å, accompanied by a nearly complete averaging of 'long' and 'short' bonds. Therefore the local symmetry at one molybdenum centre approaches closely C_{4v} symmetry, as expected for a Mo^v. The Mo–O–Mo bond angles increase slightly from 164 to 166°. By compensating each other all structural alterations described so far leave the S...S distance of 3.92 Å unchanged. Whether the observed increase in the Mo–O_i bond distances is significant remains unclear. The Mo=O_i stretching frequencies do not change upon reduction. The displacements of the molybdenum atoms within their respective MoO₆ octahedra, which cause the strongly alternating (1.80–2.02 Å) Mo–O–Mo bonds in $[\text{S}_2\text{Mo}_{18}\text{O}_{62}]^{4-}$, are generally very small in $[\text{H}_3\text{S}_2\text{Mo}_{18}\text{O}_{62}]^{5-}$. The chirality of $[\text{H}_3\text{S}_2\text{Mo}_{18}\text{O}_{62}]^{5-}$ may probably not be detected by ORD spectroscopy,¹⁸ in contrast to two-electron reduced $[\text{H}_2\text{P}_2\text{Mo}_{18}\text{O}_{62}]^{6-}$. However, the chirality of the latter, which is considerably diminished compared to $[\text{P}_2\text{Mo}_{18}\text{O}_{62}]^{6-}$, was still observed.¹⁹

Table 3 Molybdenum–oxygen bond distances (Å) in the bonds between triplets and equatorial belts in $[\text{H}_3\text{S}_2\text{Mo}_{18}\text{O}_{62}]^{5-}$

Mo(1)–O(10)	1.865(4)	Mo(4)–O(10)	1.977(4)
Mo(1)–O(11)	1.896(3)	Mo(8)–O(11)	2.005(4)
Mo(2)–O(16)	1.850(3)	Mo(9)–O(16)	1.991(3)
Mo(2)–O(15)	1.931(4)	Mo(7)–O(15)	2.003(4)
Mo(3)–O(17)	1.880(4)	Mo(6)–O(17)	1.984(4)
Mo(3)–O(18)	1.947(4)	Mo(5)–O(18)	2.023(4)
Mo(1)–O(10)–Mo(4)	151.7(2)	Mo(1)–O(11)–Mo(8)	150.5(2)
Mo(4)–O(19)–Mo(8)	154.7(2)	Mo(2)–O(15)–Mo(7)	149.4(2)
Mo(2)–O(16)–Mo(9)	153.0(2)	Mo(3)–O(18)–Mo(5)	150.1(2)

Table 4 Summary of cell data, data collection and refinement details*

Compound	1	2	3
Formula	$\text{C}_{88}\text{H}_{90}\text{KM}_{12}\text{N}_4\text{O}_{46}\text{P}_5$	$\text{C}_{124}\text{H}_{156}\text{K}_2\text{M}_{12}\text{N}_{10}\text{O}_{58}\text{P}_5$	$\text{C}_{88}\text{H}_{192}\text{M}_{18}\text{N}_9\text{O}_{62}\text{S}_2$
<i>M</i>	3284.9	4098.9	4159.5
Colour, habit	Yellow plates	Blue plates	Blue plates
Crystal size/mm	0.08 × 0.17 × 0.32	0.08 × 0.2 × 0.28	0.08 × 0.15 × 0.25
Crystal system	Triclinic	Triclinic	Monoclinic
<i>a</i> /Å	18.822(4)	16.703(3)	26.122(5)
<i>b</i> /Å	18.990(4)	16.938(3)	15.499(3)
<i>c</i> /Å	19.023(4)	17.634(4)	36.106(7)
α /°	111.27(3)	107.55(3)	—
β /°	115.55(3)	96.37(3)	105.80(3)
γ /°	90.52(3)	117.80(3)	—
<i>U</i> /Å ³	5605(2)	4016.1(14)	14 066(5)
Space group	$P\bar{1}$	$P\bar{1}$	$C2/c$
<i>Z</i>	2	1	4
<i>F</i> (000)	3224	2051	8260
<i>D</i> _c /g cm ⁻³	1.946	1.695	1.964
μ /mm ⁻¹	1.490	1.089	1.660
Lattice segment	+ <i>h</i> , ± <i>k</i> , ± <i>l</i>	+ <i>h</i> , ± <i>k</i> , ± <i>l</i>	+ <i>h</i> , + <i>k</i> , ± <i>l</i>
2 θ range/°	4–48	4–48	4–54
Reflections measured	18 683	11 671	14 000
Unique reflections	17 691	11 181	12 439
Reflections with <i>I</i> ≥ 2 σ (<i>I</i>)	11 675	7740	9157
No. variables in least squares	1347	970	807
<i>R</i> , <i>R</i> '	0.053, 0.056	0.050, 0.065	0.036, 0.045
Residual electron density/ <i>e</i> Å ⁻³	1.72	2.19	1.10

* Details in common: Siemens R3m/V diffractometer; *T* 170 K; Mo–K α radiation ($\lambda = 0.710 73$ Å); scan mode ω -2 θ ; empirical absorption correction.

It is difficult to relate the ¹⁷O and ³¹P NMR spectroscopic results of Kazansky and Fedotov²⁰ with our results. The authors deduce that the two extra electrons in $[\text{P}_2\text{Mo}_{18}\text{O}_{62}]^{8-}$ are firmly trapped by two adjacent molybdenum atoms located in both half-units of the anion. We were unable to record ¹⁷O NMR spectra of $[\text{H}_3\text{S}_2\text{Mo}_{18}\text{O}_{62}]^{5-}$. However, according to the structural data, the four extra electrons are not localised in two pairs of adjacent octahedra. Still the strongest structural changes upon reduction occur in the belts. The electron delocalisation extends very probably also into the region where the protons reside, and into the triplets, where significant structural changes were observed. Present EPR evidence is consistent with thermal delocalisation of the odd electron over the complete polyoxoanion framework in solid $[\text{NBu}^n_4]_5[\text{S}_2\text{Mo}_{18}\text{O}_{62}]^{12-}$.^{12c} Further spectroscopic and theoretical investigations are necessary to rationalise the observed structural changes.

Experimental

Synthesis.—All preparations and analytical measurements were performed under an atmosphere of purified nitrogen, unless stated otherwise.

$[\text{N}(\text{PPh}_3)_2]_3[\text{PMo}_{12}\text{O}_{40}]$. Solutions of $\text{H}_3[\text{PMo}_{12}\text{O}_{40}] \cdot x\text{H}_2\text{O}$ (5 g, 2.74 mmol) in methanol (10 cm³) and of $[\text{N}(\text{PPh}_3)_2]\text{Cl}$ (4.7 g, 8.22 mmol) in methanol (10 cm³) were combined in air. A light yellow precipitate was formed, which was filtered off, washed with methanol and dried in air. Yield 8.76 g, 93%.

$[\text{K}(18\text{-crown-6})][\text{N}(\text{PPh}_3)_2]_2[\text{PMo}_{12}\text{O}_{40}] \cdot 2\text{MeCN}$ **1**. The ion $[\text{K}(18\text{-crown-6})]^+$ (0.3 g, 0.9 mmol) was added to a solution of $[\text{N}(\text{PPh}_3)_2]_3[\text{PMo}_{12}\text{O}_{40}]$ (1 g, 0.3 mmol) in acetonitrile (50 cm³). The solution was concentrated close to saturation. Upon cooling to 0 °C yellow, cube-like crystals of **1** were formed and isolated. Yield 0.7 g, 81% (Found: C, 32.15; H, 2.85; N, 1.80. Calc. for $\text{C}_{88}\text{H}_{90}\text{KM}_{12}\text{N}_4\text{O}_{46}\text{P}_5$: C, 32.15; H, 2.75; N, 1.70%).

$[\text{K}(18\text{-crown-6})]_2[\text{N}(\text{PPh}_3)_2]_2[\text{HPMo}_{12}\text{O}_{40}] \cdot 8\text{MeCN}$ -18-crown-6 **2**. Triphenylphosphine (1.15 g, 4.35 mmol) was added to a solution of $[\text{N}(\text{PPh}_3)_2]_3[\text{PMo}_{12}\text{O}_{40}]$ (5 g, 1.45 mmol) in acetonitrile (50 cm³). The solution was refluxed for 50 h. It

Table 5 Positional parameters ($\times 10^4$) for $[\text{PMo}_{12}\text{O}_{40}]^{3-}$ with estimated standard deviations (e.s.d.s) in parentheses

Atom	X/a	Y/b	Z/c	Atom	X/a	Y/b	Z/c
Mo(1)	9 774(1)	-1 804(1)	8 368(1)	Mo(7)	4 598(1)	4 414(1)	-2 156(1)
Mo(2)	11 175(1)	-182(1)	8 925(1)	Mo(8)	3 674(1)	3 210(1)	-1 582(1)
Mo(3)	11 557(1)	-1 073(1)	10 376(1)	Mo(9)	5 790(1)	3 440(1)	-915(1)
Mo(4)	11 597(1)	1 540(1)	10 761(1)	Mo(10)	3 855(1)	3 957(1)	513(1)
Mo(5)	8 344(1)	-593(1)	7 911(1)	Mo(11)	2 888(1)	4 871(1)	-889(1)
Mo(6)	9 819(1)	1 112(1)	8 798(1)	Mo(12)	4 077(1)	6 150(1)	-1 127(1)
P(1)	0	0	0	P(2)	5 000	5 000	0
O(1)	9 647(5)	-2 617(4)	7 567(5)	O(23)	4 477(5)	4 145(5)	-3 138(4)
O(2)	11 766(5)	-263(4)	8 478(5)	O(24)	3 053(5)	2 413(4)	-2 358(5)
O(3)	12 240(4)	-1 620(4)	10 507(5)	O(25)	6 127(5)	2 678(4)	-1 332(5)
O(4)	12 298(5)	2 287(4)	11 093(6)	O(26)	3 342(5)	3 420(4)	722(5)
O(5)	7 543(5)	-867(5)	6 968(5)	O(27)	1 908(5)	4 833(5)	-1 233(5)
O(6)	9 709(5)	1 574(4)	8 180(4)	O(28)	3 615(5)	6 637(4)	-1 709(4)
O(7)	9 064(5)	-2 050(5)	8 694(5)	O(29)	5 415(5)	3 808(5)	-1 738(6)
O(8)	10 672(5)	-1 827(6)	9 247(6)	O(30)	3 858(5)	3 694(5)	-2 281(6)
O(9)	8 936(5)	-1 316(5)	7 732(5)	O(31)	5 625(5)	5 205(5)	-1 504(6)
O(10)	10 442(5)	-1 100(6)	8 246(6)	O(32)	4 069(5)	5 206(5)	-2 037(6)
O(11)	10 485(5)	396(5)	8 491(5)	O(33)	2 935(7)	3 947(6)	-1 596(6)
O(12)	11 760(5)	783(5)	9 955(5)	O(34)	3 655(6)	3 200(5)	-643(5)
O(13)	11 744(5)	-633(6)	9 749(5)	O(35)	4 637(5)	2 954(5)	-1 362(6)
O(14)	12 032(5)	1 192(5)	11 601(5)	O(36)	4 136(5)	6 708(5)	-92(5)
O(15)	10 705(5)	1 676(5)	9 775(5)	O(37)	6 685(6)	4 177(5)	-181(4)
O(16)	8 960(6)	175(4)	7 958(6)	O(38)	3 102(6)	4 408(5)	-50(5)
O(17)	12 008(6)	-230(4)	11 374(6)	O(39)	5 139(5)	6 437(5)	-806(6)
O(18)	10 893(6)	-1 441(4)	10 793(6)	O(40)	3 153(6)	5 447(5)	-1 354(5)
O(19)	10 424(7)	-572(7)	9 547(8)	O(41)	4 864(8)	4 307(8)	-786(8)
O(20)	9 392(8)	-657(7)	9 240(8)	O(42)	4 942(7)	5 275(7)	-696(7)
O(21)	10 453(7)	454(7)	9 744(8)	O(43)	4 162(8)	4 472(7)	-382(8)
O(22)	10 612(7)	-268(7)	10 666(8)	O(44)	5 663(7)	4 538(7)	172(8)

Table 6 Positional parameters ($\times 10^4$) for $[\text{HPMo}_{12}\text{O}_{40}]^{4-}$ with e.s.d.s in parentheses

Atom	X/a	Y/b	Z/c
Mo(1)	-76(1)	7 023(1)	9 848(1)
Mo(2)	2 073(1)	7 006(1)	9 957(1)
Mo(3)	-1 236(1)	2 708(1)	8 257(1)
Mo(4)	793(1)	4 707(1)	8 184(1)
Mo(5)	-1 354(1)	4 712(1)	8 116(1)
Mo(6)	2 113(1)	4 937(1)	10 049(1)
O(1)	-111(5)	7 958(5)	9 773(4)
O(2)	3 034(5)	7 933(5)	9 919(4)
O(3)	-1 854(5)	1 630(5)	7 451(4)
O(4)	1 150(7)	4 570(5)	7 342(4)
O(5)	-1 973(5)	4 583(5)	7 237(4)
O(6)	3 103(5)	4 927(5)	10 077(4)
O(7)	1 137(6)	7 295(7)	9 690(4)
O(8)	-647(7)	6 089(5)	8 731(5)
O(9)	554(6)	7 519(7)	11 011(4)
O(10)	-1 240(7)	6 336(5)	10 057(5)
O(11)	1 613(5)	4 576(5)	8 904(4)
O(12)	-210(5)	4 897(5)	7 867(6)
O(13)	1 563(6)	6 084(5)	8 811(4)
O(14)	-171(5)	3 386(6)	7 951(6)
O(15)	-2 119(6)	2 506(7)	8 908(5)
O(16)	-1 725(5)	3 419(5)	7 924(6)
O(17)	2 546(6)	6 261(5)	10 202(4)
O(18)	-2 167(7)	4 626(5)	8 791(5)
O(19)	-683(8)	5 301(8)	9 623(7)
O(20)	-260(8)	4 507(8)	9 062(6)
O(21)	813(9)	5 294(8)	9 692(7)
O(22)	-629(8)	3 888(8)	9 721(7)
P	0	5 000	10 000

turned rapidly from yellow to green and finally to dark blue. The solvent was evaporated and methanol was added to dissolve triphenylphosphine oxide and unreacted triphenylphosphine. The remaining dark blue powder was filtered off and dried *in vacuo*, yield 3.5 g, 70%. It was dissolved (1 g, 0.3 mmol) in acetonitrile (50 cm³), $[\text{K}(18\text{-crown-6})]\text{Cl}$ (0.3 g, 0.9 mmol)

was added and the solution concentrated. After 3 d at 0 °C cube-like blue-black crystals of compound **2** appeared. They deteriorated immediately outside the mother-liquor. Yield 0.72 g, 58%.

$[\text{NBu}^n_4]_4[\text{S}_2\text{Mo}_{18}\text{O}_{62}]$. This salt was prepared according to Hori *et al.*¹⁸

$[\text{NBu}^n_4]_5[\text{H}_3\text{S}_2\text{Mo}_{18}\text{O}_{62}]\cdot 4\text{MeCN}$ **3**. Triphenylphosphine (1.4 g, 5.3 mmol) was added to a solution of $[\text{NBu}^n_4]_4[\text{S}_2\text{Mo}_{18}\text{O}_{62}]$ (5 g, 1.33 mol) in acetonitrile (50 cm³). The solution was refluxed for 72 h. During this time it changed from orange to green and finally to deep blue. The solution was carefully evaporated to dryness. The remaining blue-black powder was filtered off, washed with methanol and recrystallised from acetonitrile to yield 4.6 g (85%) of compound **3** as well formed crystals (Found: C, 21.20; H, 4.10; N, 2.05. Calc. for $\text{C}_{88}\text{H}_{192}\text{Mo}_{18}\text{N}_9\text{O}_{62}\text{S}_2$: C, 25.40; H, 4.70; N, 1.70%).

Analyses.—In order to determine the molybdenum(v) content in the reduced polyoxometalates a solution of compound **2** (0.023 g, 5.6×10^{-6} mol) in acetonitrile (50 cm³) was titrated with an aqueous solution of cerium(IV) sulfate (0.01 mol dm⁻³). A 1.2 cm³ volume of this standard solution was necessary to change the molybdate solution from blue to light yellow. This is equivalent to 2.16 molybdenum(v) atoms per formula unit. The same procedure was applied to compound **3** (0.050 g in 150 cm³ CH₃CN) and gave 4.16 molybdenum(v) atoms per formula unit.

Physical Measurements.—Infrared spectra were recorded using a Bruker IFS 113v spectrometer and the KBr technique, UV/VIS/near-IR spectra in the range 190–1400 nm on a Shimadzu 3100 instrument.

Structural Analyses and Refinements.—Details of X-ray experimental conditions, all data, data collection and refinement parameters are summarised in Table 4. Direct methods were followed by standard full-matrix least-squares procedures using the program system SHELXTL PLUS²¹ and applying the weighting scheme $w = 1/[\sigma^2(F_o) + gF_o^2]$ with

Table 7 Positional parameters ($\times 10^4$) for $[\text{H}_3\text{S}_2\text{Mo}_{18}\text{O}_{62}]^{5-}$ with e.s.d.s in parentheses

Atom	X/a	Y/b	Z/c	Atom	X/a	Y/b	Z/c
Mo(1)	4691(1)	-992(1)	1091(1)	O(12)	4143(2)	-183(3)	844(1)
Mo(2)	5400(1)	908(1)	1148(1)	O(13)	5177(2)	-199(3)	934(1)
Mo(3)	4045(1)	954(1)	1023(1)	O(14)	4673(2)	1281(3)	885(1)
Mo(4)	4146(1)	-1672(1)	1898(1)	O(15)	5393(2)	1860(2)	1491(1)
Mo(5)	3462(1)	255(1)	1842(1)	O(16)	5921(1)	402(2)	1540(1)
Mo(6)	4206(1)	2340(1)	1903(1)	O(17)	4158(2)	1849(2)	1387(1)
Mo(7)	5567(1)	2332(1)	2028(1)	O(18)	3641(2)	392(3)	1334(1)
Mo(8)	4372(1)	-1682(1)	2964(1)	O(19)	4905(2)	-1877(2)	2049(1)
Mo(9)	3687(1)	236(1)	2909(1)	O(20)	3535(1)	-952(2)	1777(1)
S(1)	5115(1)	301(1)	3060(1)	O(21)	4173(1)	-1636(2)	2426(1)
O(1)	4616(2)	-1761(3)	750(1)	O(22)	3543(1)	108(2)	2370(1)
O(2)	5744(2)	1311(3)	853(1)	O(23)	3749(2)	1396(2)	1940(1)
O(3)	3566(2)	1350(3)	650(1)	O(24)	4873(2)	2835(2)	1894(1)
O(4)	3872(2)	-2653(2)	1782(1)	O(25)	5622(2)	2451(2)	2556(1)
O(5)	2803(2)	392(3)	1682(1)	O(26)	6060(2)	1385(2)	2147(1)
O(6)	3790(2)	3172(3)	1769(1)	O(27)	3789(1)	-969(2)	2983(1)
O(7)	5940(2)	3166(2)	1961(1)	O(28)	4797(1)	301(2)	1512(1)
O(8)	4161(2)	-2670(2)	3035(1)	O(29)	4615(1)	-146(2)	2885(1)
O(9)	3070(2)	390(3)	2956(1)	O(30)	4913(1)	1198(2)	2071(1)
O(10)	4258(2)	-1359(2)	1395(1)	O(31)	4438(1)	-143(2)	2033(1)
O(11)	5290(2)	-1363(2)	1486(1)				

$g = 0.0004$ for compounds **1** and **3**, 0.0005 for **2**. All non-hydrogen atoms were refined anisotropically. Hydrogen atoms were included in calculated positions with overall $U_{\text{iso}} = 0.08 \text{ \AA}^2$. Atomic coordinates for the atoms in the anions are given in Tables 5–7. The structures of **1** and **2**, when refined in space group $P\bar{1}$, showed disorder of the polymolybdate anions (see discussion above) due to the presence of an inversion centre. We also tried to refine the structures in the acentric space group $P1$ by placing metal atom frameworks with T_d symmetry at the origin and restraining their interatomic distances. However, these refinements did not converge. Apart from the anions, the remaining parts of the unit cells are not disordered. This underlines the correct choice of space group ($P\bar{1}$) for **1** and **2**. In **3** one NBu_4^+ is partly disordered.

Additional material available from the Cambridge Crystallographic Data Centre comprises H-atom coordinates, thermal parameters and remaining bond lengths and angles.

References

- M. T. Pope, *Heteropoly and Isopoly Oxometalates*, Springer, Berlin, New York, 1983.
- M. T. Pope and A. Müller, *Angew. Chem.*, 1991, **103**, 56; *Angew. Chem., Int. Ed. Engl.*, 1991, **30**, 34.
- M. T. Pope and A. Müller, *Polyoxometalates: from Platonic Solids to Antiretroviral Activity*, Kluwer, Dordrecht, 1994.
- P. Le Maguerès, L. Ouahab, S. Golhen, D. Grandjean, O. Peña, J.-C. Jegaden, C. J. Gomez-Garcia and P. Delhaès, *Inorg. Chem.*, 1994, **33**, 5180 and refs. therein.
- J. N. Barrows, G. B. Jameson and M. T. Pope, *J. Am. Chem. Soc.*, 1985, **107**, 1771.
- J. N. Barrows and M. T. Pope, *Adv. Chem. Ser.*, 1990, **226**, 403.
- A. Müller, E. Krickemeyer, M. Penk, V. Wittneben and J. Döring, *Angew. Chem.*, 1990, **102**, 85; *Angew. Chem., Int. Ed. Engl.*, 1990, **29**, 88.
- N. Casañ-Pastor, P. Gomez-Romero, G. B. Jameson and L. C. W. Baker, *J. Am. Chem. Soc.*, 1994, **33**, 5180.
- I. Kawafune and G. Matsubayashi, *Chem. Soc. Jpn. Chem. Lett.*, 1986, 1503.
- I. Kawafune, *Chem. Soc. Jpn. Chem. Lett.*, 1989, 185.
- I. Kawafune and G. Matsubayashi, *Inorg. Chim. Acta*, 1991, **188**, 33.
- (a) R. Contant and J. M. Fruchart, *Rev. Chim. Miner.*, 1974, **11**, 123; (b) J. N. Barrows and M. T. Pope, *Inorg. Chim. Acta*, 1993, **213**, 91; (c) J. B. Cooper, D. M. Way, A. M. Bond and A. G. Wedd, *Inorg. Chem.*, 1993, **32**, 2416; (d) U. Körtz and M. T. Pope, *Inorg. Chem.*, 1994, **33**, 5643.
- C. Rocchiccioli-Deltcheff, R. Thouvenot and R. Franck, *Spectrochim. Acta, Part A*, 1976, **32**, 587; C. Rocchiccioli-Deltcheff, M. Fournier, R. Franck and R. Thouvenot, *Inorg. Chem.*, 1983, **22**, 207.
- H. T. Evans, jun. and M. T. Pope, *Inorg. Chem.*, 1984, **23**, 501.
- H. Ichida, A. Kobayashi and Y. Sasaki, *Acta Crystallogr., Sect. B*, 1980, **36**, 1382 and refs. therein.
- S. W. Zhang, G. Q. Huang, Y. G. Wei, M. C. Shao and Y. Q. Tang, *Acta Crystallogr., Sect. C*, 1993, **49**, 1446.
- J.-M. Fruchart and P. Souchay, *C. R. Hebd. Seances Acad. Sci., Ser. C*, 1968, **266**, 1571.
- T. Hori, O. Tamada and S. Himeno, *J. Chem. Soc., Dalton Trans.*, 1989, 1491.
- J. F. Garvey and M. T. Pope, *Inorg. Chem.*, 1978, **17**, 1115.
- L. P. Kazansky and M. A. Fedotov, *J. Chem. Soc., Chem. Commun.*, 1980, 644.
- G. M. Sheldrick, SHELXTL PLUS, Siemens Analytical Instruments, Madison, WI, 1990.

Received 7th February 1995; Paper 5/00715A